

# Wafer-scale fabrication and assembly method of multichannel microelectrode arrays for ECoG application

Ho-Kun Sung<sup>1</sup>, Meng Zhao<sup>\*2</sup>, Cong Wang<sup>\*3</sup>, Alok Kumar<sup>3</sup>, Tian Qiang<sup>3</sup>, Zhong-Liang Zhou<sup>3</sup>, and Dan-Qing Zou<sup>3</sup>

<sup>1</sup>Korea Advanced Nano Fab Center (KANC), Suwon, 443270, Republic of Korea

<sup>2</sup>Jiangsu Key Laboratory of Micro and Nano Heat Fluid Flow Technology and Energy Application, School of Mathematics and Physics of Mathematics and Physics, Suzhou University of Science and Technology, Suzhou 215009, China

<sup>3</sup>School of Electronics and Information Engineering, Harbin Institute of Technology, Harbin 150001, China

E-mail: mzhao@usts.edu.cn (Meng Zhao) and kevinwang@hit.edu.cn (Cong Wang)

## Abstract

High density electrocorticography (ECoG) based microelectrode arrays (MEAs) are fabricated to timely record the neural activities to provide the fundamental understanding in neuroscience and biomedical engineering. This paper is aimed to introduce device-based concept and wafer-scale fabrication process for MEAs. High resistive silicon wafer is used as a substrate to minimize substrate losses and increase Q-factor of the device. In addition flexible and biocompatible polyimide is applied on MEAs to bear all possible stress and strain. Detailed fabrication key techniques including surface treatment, polyimide stability measurement, evaporation process, and curing conditions have been discussed thoroughly. Moreover, the precise advanced fabrication process was helped to extract 25 groups of MEAs from a single 6-inch silicon wafer. Each single MEA is consisting of 60 channels with compact size, so that the testing skull can be fully covered with more recording sites and the neural signal can be recorded more thoroughly. Moreover, the fabricated polyimide-based MEAs are also surface-mounted on a well-packaged by printed circuit boards (PCBs) via slot-type connector without any additional wire bonding to make the signal recording process easier. The proposed MEAs could be remained at the skull and the connector and PCBs can be disassembled apart, so that the testing sample will be suffered less. To verify the robustness of the fabricated MEAs, the impedance properties are characterized using electrochemical impedance spectroscopy. The measured results indicate average impedance of  $12.3 \pm 0.675 \text{ k}\Omega$  at 1 kHz. 10 groups of MEAs are sampling tested and over 90% of the total 60-channels per 1-MEAs operated efficiently. This work provides step-by-step fabrication technology, assembly method, and measurement process, which could be beneficial for the researchers that are still facing potential wafer-scale fabrication issues of MEAs.

Keywords: Microelectrode arrays, wafer-scale fabrication, multichannel, neuronal recordings.

## 1. Introduction

Electrical activities recording of neural cell networks can provide a wealth of information concerning with the physiology as well as physiological degenerations that may cause diseases, such as Parkinson's or Alzheimer's [1, 2]. Microelectrode

arrays (MEAs) have been adopted to monitor neural signal for a long time at regular intervals through electrocorticography (ECoG) methods. This method provides an advanced understanding about the functioning of the brain activities [3]. Flexibility and biocompatibility are the primary condition related with practical application of MEAs for recording in vivo

data from the subject on long term basis [4]. These conditions also allow the MEAs to be placed directly on the skull to interface with nervous system. Commonly, the polyimide is applied as the base material, offering an excellent biocompatibility and high flexibility for the manufacturing of MEAs. In the past few years, the flexible MEAs have been consistently developed to stimulate and record from multiple neurons [5-8]. There are several high sensitive MEAs have been developed using micro-electromechanical systems (MEMS) [9-11], complementary metal-oxide-semiconductor (CMOS) [12], and lab-on-chip micro-fabrication techniques [13, 14] to fabricate large numbers of electrode arrays over a small area. Moreover, to enable simultaneous and multisite recording from a large number of individual neurons, electrode is preferred to be operated at high spatiotemporal resolution [15]. Furthermore, a precise wafer-scale process can offer to fabricate MEAs with excellent uniformity, enhanced quality, and tolerance to achieve high reliability. The current research is focused to fabricate MEAs with advance micro-fabrication technique to lower the production cost with higher yield. The large wafer-scale micro-fabrication can greatly reduce manufacturing cost due to the possibility of mass production [16].

In this work, we apply the 6-inch high resistive silicon wafer as the substrate and combine it with flexible polyimide to manufacture 25 MEAs on single wafer through mass production. There are several key techniques such as surface treatment, evaporation process, and curing conditions are adopted during micro-fabrication process. The MEAs are designed to offer high spatiotemporal resolution through 60 recording channels, aiming to fulfill the sensor condition of high sensitive and selective in the recording of neural signals. Moreover, the fabricated MEAs are surface-mounted on well packaged printed circuit boards (PCBs) via slot-type connector to facilitate the signal recording process. Such connectors and PCBs can be disassembled apart, if the signal recording is not acquired. This circuitry advancement relieves the patient to carry extra weight of connector and PCBs and provides the possibility to remain the flexible MEAs on the *in vivo* test until next-round recording. The reliability of assembled MEAs have been characterized via electrochemical impedance spectroscopy. In summary, the whole process including step-by-step fabrication technology, assembly method, and measurement process are also discussed in this work. This discussion could be beneficial for the researchers who are facing potential wafer-scale fabrication issues of MEAs.

## 2. Experimental Details

The fabrication schematic of the proposed flexible and multichannel MEAs is shown in Figure 1. Based on the wafer-scale micro-fabrication, the MEAs are processed and fabricate with the following 7 steps. Step 1: The silicon substrate is firstly dipped into the 10% HF solution to remove the existed oxide. Afterwards, the substrate is prepared for plasma

treatment using  $O_2/H_2$  with a RF power of 650 W, chuck temperature of 80 °C, chamber pressure of 2 Torr, and process time of 30 s. This process helps to deposit Al sacrificial layer with high adhesion. Substrate roughness with a root mean square value (RMS) of 8.64 nm is shown in Figure 2. This accurate surface roughness helps to enhance the adhesion between silicon substrate and Al metal layer. Step 2: Al sacrificial layer, with a thickness of 3  $\mu m$ , is deposited through e-beam processes. Step 3: The most commonly used base materials of MEAs named non-photosensitive polyimide (HD Microsystems, PIX1400) is spin-coated on the Al layer. The polyimide is deposited three times as 3  $\mu m$  in each time through manual spin-coater with revolutions per minute (RPM) of 500/3000/500 and corresponded time of 10/40/5 s, respectively. After that, soft baking is done under 100 °C for 3 mins, followed by curing process under 300 °C for 3 mins in conventional oven. The accumulated thickness of 9  $\mu m$  is achieved during the whole process. This much polyimide thickness could just relieve the tensile stress, which will be proceed from the coming metallization process to overcome the potential rolling issue, make the film planarization and easy to delivery. However, if the polyimide film is thicker than 9  $\mu m$ , it will bring a consequent adhesion problem when attaching the film onto the mouse skull. Therefore, the thickness of the polyimide is just fixed to 9  $\mu m$  to minimize both of these two issues. Step 4: Photolithography process is employed to pattern the polyimide with specific pattern and followed with the curing process in a condition of 90 °C for 30 mins and 125 °C for 60 mins separately, in order to achieve a stable height and shape with excellent aspect ratio. Moreover, the polyimide surface is treated with inductively coupled plasma etching process under the condition of chamber pressure of 450 mTorr, coil power of 650 W, a  $CF_4$  flow of 8 sccm, and an  $O_2$  flow of 72 sccm.

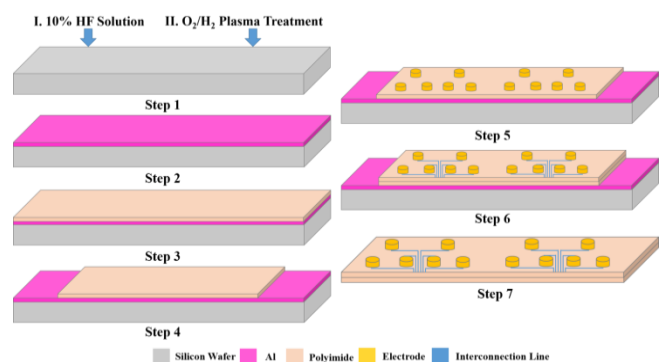


**Figure 1.** The fabrication schematic of the proposed flexible polyimide-based multi-channel MEAs.

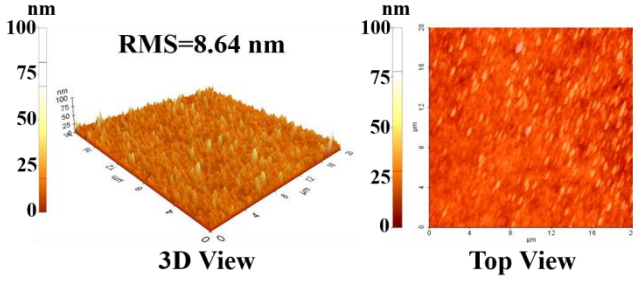


**Figure 2.** Surface morphology of the silicon wafer after  $O_2/H_2$  plasma treatment.

The adhesion between the first polyimide layer and Cr/Pt metal layer, as well as the second polyimide layer, could be promoted with a RMS value of 14.01 nm as demonstrated in Figure 3. Step 5: The recording electrode network of 60-channels is formed by photolithography, in which the Cr/Pt (15/150 nm) metal layer is evaporated with an appropriate deposition rates of 3 Å/s and 3 Å/s, respectively and then lift-off process is executes. In lift-off process the pressure of 3 MPa is used to clean the fabricated devices with acetone treatment for 60 s, followed by IPA treatment for 30 s, and finally DI-water treatment for 60 s. Step 6: The wafer is sequentially fabricated through the second polyimide patterning process, similar to Step 3. The wafer is masked using photoresist to define interconnection lines and pads of the structure. After that, a 15/150 nm-thick Cr/Pt metal layer is formed by using e-beam evaporator with a deposition rate of 3 Å/s and 3 Å/s, respectively. At last, the mask of interconnection lines and pads is stripped by lift-off process using acetone/IPA/DI, respectively. Step 7: Wet etching process with Al etchant is applied to fully remove the Al sacrificial layer and finally the expected MEAs can be obtained.

Figure 4 shows the designed and fabricated structures of a single MEAs as well as a fully processed 6-inch silicon wafer. Three parts including recording sites, interconnection lines, and interconnection pads are designed to realize the final MEAs.

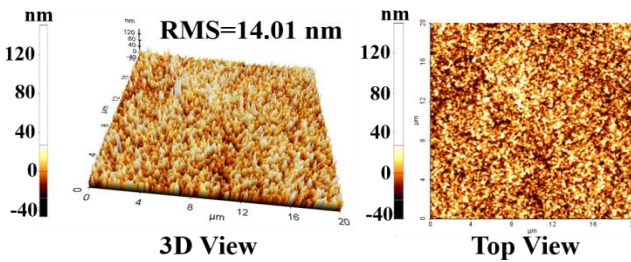


**Figure 3.** Surface morphology of the polyimide wafer after  $O_2$  plasma treatment.

Recording sites are arranged in a high spatiotemporal resolution while maintaining a compact area. The interference between the adjacent electrodes can be efficiently minimizes through optimizing MEAs structure. Interconnection lines are

clearly demonstrated without any shorting points, which are guaranteed to transfer reliable signal from the recording electrode to the detection equipment.

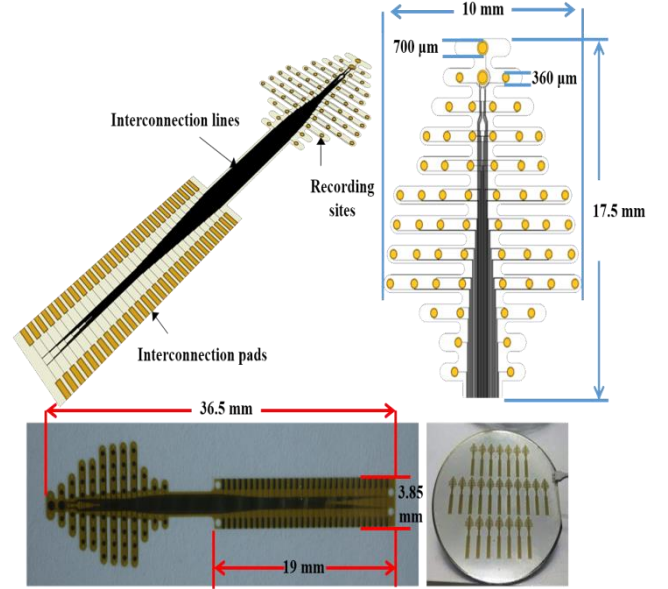


**Figure 4.** The designed and fabricated structure of a single MEAs and a fully processed 6-inch silicon wafer.

Moreover, interconnection pads are particularly added in the proposed work to connect with slot-type connector and the fabricated devices. The advanced fabrication method is produced to fabricate 25 flexible MEAs on a single silicon wafer. The maximally exploitation due to wafer edge defection and fabrication tolerance is considered cautiously.

The fully assembled flexible MEAs and its schematic plot (a), side view (b), and top view (c) are shown in Figure 5. The practical surface mounted device is fabricated with a slot-type connector without any additional bonding wires. This fabricated formation prevents the device from electrical interconnection failure, which may cause by skull tissues during *in vivo* tests. The flexible PCB (FPCB, (polyimide based structure) is used to support MEAs electrodes and provides protection from physical damage. The top and bottom PCBs are processed with a connector socket on the front side and interconnection pads on the backside. The FPCB is connected with top and bottom PCBs through a V-cut, that can be easily removed during *in vivo* testing. Usually, the skull signal could be recorded for a long time and sometimes several rounds of recording is also preferred to provide an accurate and reliable measurement results. Therefore, the top PCB, bottom PCB, and slot type connector are designed to be disassembled apart during *in vivo* recording process. This innovated circuitry helps the potential patient to relieve from acute suffering caused by the additional weight of the top and bottom PCB. Moreover, the scalp surgery is also not required during the next-round of measurement. This

innovative process can help to save cost and reduce the complexity along with patient personal releive.

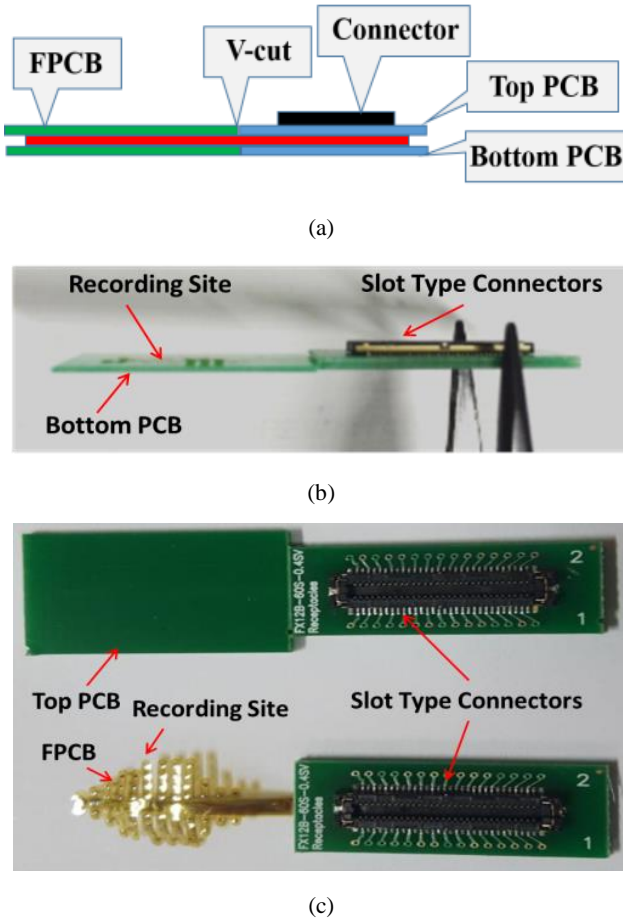


**Figure 5.** Images of the flexible MEAs mounted on the surface of PCB, (a) schematic demonstration, (b) side view, and (c) top view.

### 3. Result and Discussion

To investigate the functionality and reliability of the fabricated MAEs, the assembled MEAs are suspended in the air and the phosphate-buffered saline (PBS) solution, which is used as a reference ground to circuit. The electric current of each individual channels are characterized by electrochemical impedance spectroscopy. The detailed measurement setup is demonstrated in Figure 6, which is comprised of a signal recording system, bibulous paper, assembled MEAs, PBS solution, and reference ground.

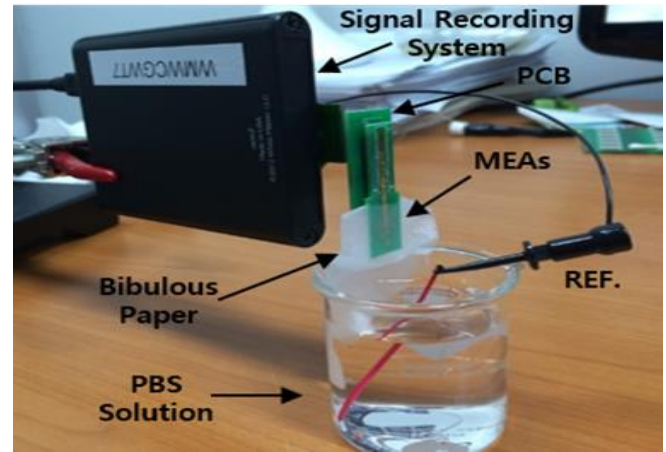


**Figure 6.** Measurement setup of the packaged MEAs.

Whenever a metal is immersed in an electrolyte, an excess concentration of electrons is formed on its surface. The interface between electrode and electrolyte remains electrically neutral and a cloud of ions form in the electrolyte adjacent to the electrode surface [17]. As long as the frequency signal is introduced, electrons will transfer through the electrode surface and a charge transfer resistance is generated. Prior to the electrons reach at the electrode-electrolyte double layer junction, the currents need to overcome the ohmic resistance of the bulky Cr/Pt electrode. The whole testing environment can be described through Randles circuit analysis as shown in Figure 7. The Randles circuit is comprised of a charge-transfer resistor  $R_{el}$  and a double layer capacitor  $C_{el}$  in parallel, cascading with the equivalent resistor of electrolyte itself  $R_{Met}$  and electric circuit path  $R_{Spread}$ . Due to the very large capacity  $C_{el}$ ,  $R_{el}$  is assumed to be small in relation and can be neglected for further study, therefore the capacity can be modelled by a constant phase element  $C_{PE}$ .

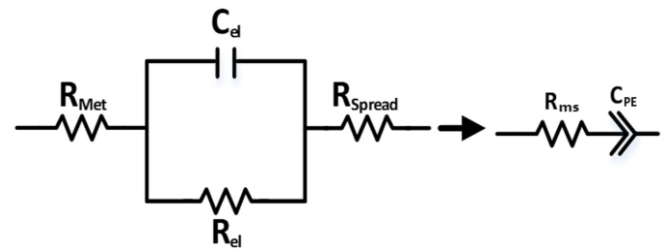


**Figure 7.** Schematic circuit of electrolyte and electrode interface.

Furthermore,  $R_{met}$  and  $R_{spread}$  are connected in series and can be replaced by single resistor  $R_{ms}$ . Then after the simplification of the basic equivalent circuit, the impedance of the complete electrochemical cell can be represented and reproduced as [18],

$$Z = Z_{PE} + Z_{ms} = \frac{1}{(Q2\pi f)^n} + R_{Met} + R_{Spread}$$



Where,  $Q$  is the double layer interface capacity in  $\mu\text{F}$ ,  $f$  is the input frequency, and  $n$  is dimensionless. The relationship between impedance  $Z$  and input frequency  $f$  is inversely proportional, indicating a criteria standard to be followed by the measurement impedance results of MEAs. The software nanoZ has been used to measure the data recording and frequency setup of the signal generator.

The impedance measurement of individual channel of each MEA is important to analyze the signal to noise ratio. The mean value of measured impedance with error bar for the single channel between frequency ranges of 1 kHz to 2 kHz is shown in Figure 8. The observed results of random single channel indicate impedance magnitude of  $145.6 \pm 5.4 \text{ k}\Omega$  at 100 Hz and  $12.3 \pm 0.675 \text{ k}\Omega$  at 1 kHz, respectively. The measured results show excellent signal to noise ration and high functionality of the assembled MEAs. In this work, 10 channels of individual MEAs are randomly chosen to implement the impedance test. The measured impedance results of all 10 channel are almost the same under 1 kHz and slight difference is emerged between 1 kHz to 2 kHz as demonstrated in inset image of Figure 8. This fruitful outcome proves a high consistency in each individual channel. Moreover, each testing channels operates efficiently with no short circuiting and interference. The high correlation between 10 channels measurement results verify the reliability and effectiveness of the advanced micro-fabrication process.

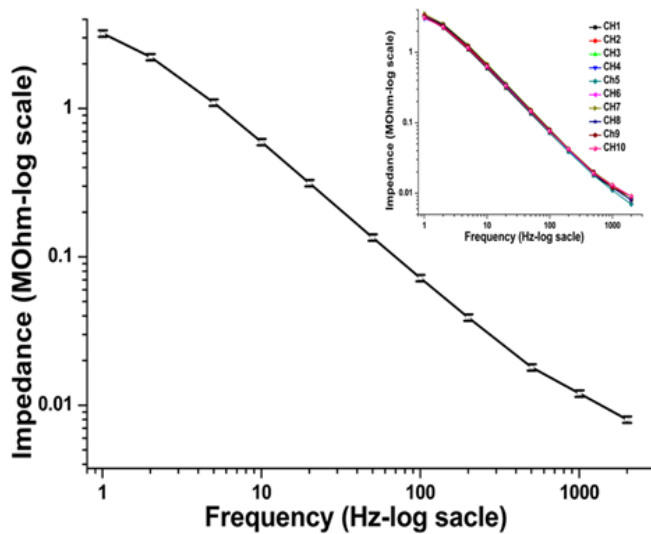


**Figure 8.** Measured impedance with error bars of single random channels of MEAs, and the inset image shows the measurement impedance properties of 10 random channels.

Reliability of a device is important for the feasibility of mass-production. It can be guaranteed for high yielding and cost-effective. The reliability of the fabricated MEAs is evaluated through driven response. The ECoG channel yield of 60 channels MEAs is shown in Figure 9. Measurement is implemented in air for all 60 channels of 10 individual MEAs, and the driven response of each MEAs has been statistically

obtained. The channels that cannot be driven may due to the issues of the fabrication failure, leakage through the polymeric encapsulation or electronic shortage. Maximum ECoG channel yield of 100% at E.7 and minimum channel yield of around 91% at E.9 can be successfully achieved for MEAs. Based on the overall statistic data, over 90% of 60 channels per 1-MEAs is normally operated, proving the excellent reliability of the fabricated MEAs and the feasibility for mass production. The proposed wafer-scale fabricated MEAs is cost-effective due to the high yield percentage and it can be regarded as a promising candidate to assist more researchers and doctors for further understanding the mechanism of neuron networks. Additionally, it also benefits for the patient to treat them with cost effective and less painful instruments.

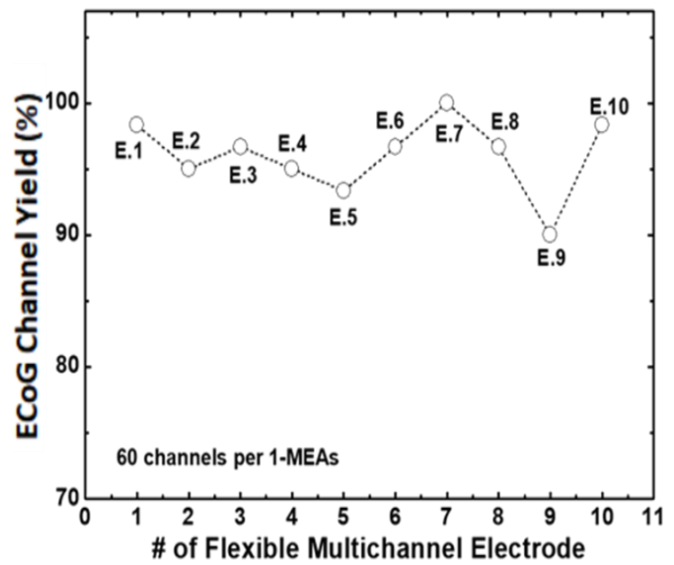


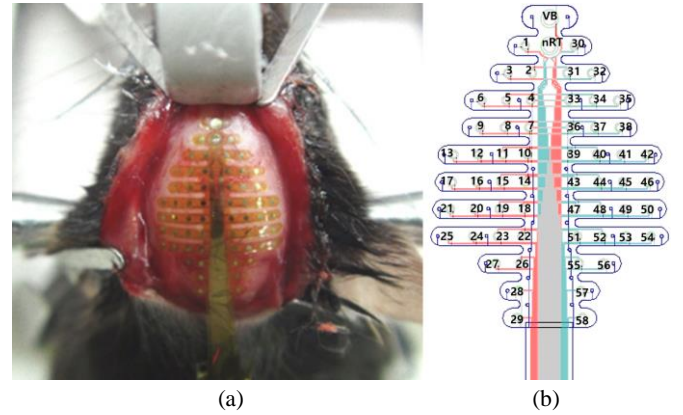
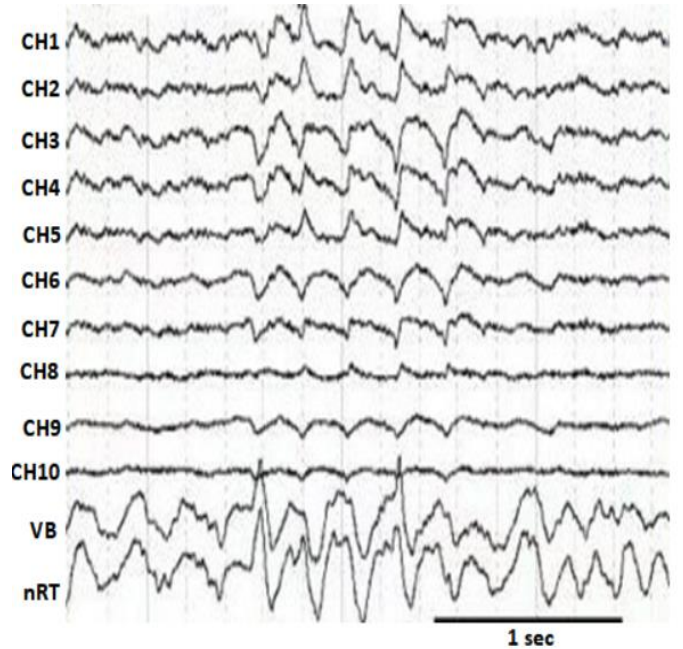
**Figure 9.** The ECoG channel yield measured from 60-channels per 1-MEAs.

As compared with other reported literatures [8, 19, 20, 21, 22] as shown in Table 1, the proposed electrode with active area dimensions of  $384650 \mu\text{m}^2$  for first electrode,  $101736 \mu\text{m}^2$  for second electrode, and the average output impedance of  $12.3 \text{ k}\Omega$  at 1 kHz is achieved for better signal acquisition with low noise and sufficient flexibility, much smaller than  $600 \text{ k}\Omega$  required by implantation [23]. The obtained results of the fabricated MAE electrodes are showing almost two order lower impedance magnitude with superior signal to noise ratio. When the size of the electrode increase, the overall structure impedance is also increases. Through comparing these obtained results, it can be concluded that there should be a trade-off between the performance of signal to noise ratio and size of electrode when facing a practical application [21].

**Table 1:** Performance comparison of the proposed MEA with several reported MEAs

Paper	Material Used for Electrode	First Electrode Size ( $\mu\text{m}^2$ )	Second Electrode Size ( $\mu\text{m}^2$ )	Average Output Impedance at 1 kHz
[8]	PMMA	70650	7850	22.7 k $\Omega$
[19]	Carbon Nano-Tubes	706.5	-	37 k $\Omega$
[20]	Gold	14000	-	1 M $\Omega$
[21]	PEDOT-pTS	413	-	45 k $\Omega$
[22]	ITO	240000	-	15 k $\Omega$
<b>This paper</b>	<b>Polyimide</b>	<b>384650</b>	<b>101736</b>	<b>12.3 k<math>\Omega</math></b>

*In vivo* test on the cerebral cortex of hybrid adult male mouse (C57BL/6J - 129S4/SvJae hybrid mice (12~15 weeks old)) is conducted to measure brain signal. The mouse is anesthetized with ketamine (120 mg/kg i.p.) and xylazine (6 mg/kg, i.p.) cocktail. The effect of anesthesia is surveillance during entire testing. Under anesthetic condition, the mouse is placed onto the stereotaxic apparatus (David Kopf Instruments, Model 902, Calif, USA). The ears bars are placed in the mouse's ear canal and tightening it carefully. The eyes can be covered with biocompatible jelly (e.g., petroleum jelly) to keep the eyes from drying up by the surgery light. After moisturizing the mouse's head with 70% ethanol, the fur is shaved off from its head. And then 2% of lidocaine hydrochloride is injected for local anesthesia. The head is incised about 2.5 cm with a scalp and the skin is pinched with micro-clamps (Fine Science Tools, Inc., 18052-03, Calif, USA) to keep the incision wide open. After that, the remaining tissues and membrane are removed from the skull by using sterilized cotton swabs. Finally, the bregma point is marked and the electrode is placed on the cortex. Before locating it onto the cerebral cortex, the electrode is primarily swabbed clean with alcohol and kept completely dry in order to obtain a better adhesion. The MEAs remains to be fixed on the cerebral cortex by van der Waals force, and an image of the *in vivo* test is demonstrated in Figure 10 (a). The electrode array has a Christmas tree structure with twelve branches on each side, and each branch has several electrical contact points, covering the exposed skull in an evenly distributed manner (Figure 10 (b)). It can be observed that the MEAs are well-arranged and conformed with the cerebral cortex ready for the signal recording after the mice gets habituated. The CH1-CH10 represent output of 10 channels among the fabricated high-density mouse EEG electrodes, VB and nRT represent the data from two big electrodes used for grounding purpose. Absence seizure is recorded on mouse skull with MEAs array by systemic administration of 50 mg/kg  $\gamma$ -butyrolactone (GBL) to induce bilaterally synchronous spike wave density (SWD). Sample traces of EEG with SWD episode are exhibited in Figure 11 and the SWDs robustly occurred in GBL model. The absence seizure is observed in all channels, and it is noticeable that strong signals are detected favorably in the parietal and frontal cortex.

**Figure 10.** Images of the microelectrode, (a) flexible MEAs mounted on the skull of adult male mouse and (b) arrangement of the high-density mouse EEG electrodes.**Figure 11.** A sample trace of EEG experiencing absence seizure induced by intraperitoneal injection of GBL. The number follows the channel montage defined in Fig. 10 (b).

#### 4. Conclusions

A wafer-scale fabrication and assembly method of flexible polyimide-based MEAs with 60 channels are proposed. Key fabrication techniques are introduced specifically to demonstrate the process flow with clear conditions and 25 MEAs is fabricated on a single 6-inch silicon wafer. FPCB and slot-type connector are applied to provide an surface-mounted assembling without additional wire-bonding process and an easier signal recording method for the fabricated MEAs. Evaluation through electrochemical impedance spectroscopy is performed on 10 MEA samples. Impedance proves the assembled MEAs with excellent robustness, which could be applied to simultaneously record neuron network with high selectivity and high sensitivity from multiple neurons. Reliability test and outstanding yield can significantly lower the price and give a chance for the proposed MEAs to pursuing a commercial success in the future biomedical market. *In vivo* test on the skull of the adult male mouse is finally proceeded to prove the conformation with the skull ready for the signal recording.

#### Acknowledgements

This work is supported by the General Financial Grant from the China Postdoctoral Science Foundation (2017M611367), the Heilongjiang Postdoctoral Fund (LBH-Z17056), the National Natural Science Foundation of China (61901206, 51502186), the Fundamental Research Fund for the Central Universities, and Zhejiang Lab (2019MC0AB03).

#### References

- [1] Kim R Y, Joo S H, Jung H J, Hong N R and Nam Y K 2014 *Biomedical Engineering Letters* **4** 129-141
- [2] Wei W J, Song Y L, Wang L, Zhang S, Luo J P, Xu S W and Cai X X 2015 *Microsystems & Nanoengineering* **1** 1-6
- [3] Buzsaki G, Anastassiou C A and Koch C 2012 *Nature Reviews Neuroscience* **13** 407-420.
- [4] Obien M E J, Deligkaris K, Bullmann T, Bakkum D J and Frey U 2015 *Frontiers in Neuroscience* **6** 1-30.
- [5] Marton G, Orban G, Kiss M, Fiath R, Pongracz A and Ulbert I 2015 *PLOS ONE* **8** 1-16
- [6] Jackel D, Bakkum D J, Russell T L, Muller J, Radivojevic M, Frey U, Franke F and Hierlemann A 2017 *Scientific Reports* **7** 1-17
- [7] Giovangrandi L, Gilchrist K H, Whittington R H and Kovacs G T A 2006 *Sensors and Actuators B* **113** 545-554
- [8] Xie K, Zhang S, Dong S, Li S, Yu C, Xu K, Chen W, Guo W, Luo J and Wu Z 2017 *Scientific Reports* **7** 1-8
- [9] Sung H K, Lee H K, Wang C and Kim N Y 2017 *Journal of Nanoscience and Nanotechnology* **17** 2582-2584
- [10] Seymour J P, Wu F, Wise K D and Yoon E 2016 *Microsystems & Nanoengineering* **3** 1-16
- [11] Jiang X, Sui X H, Liu Y L, Yan Y, Zhou C Q, Li L M, Ren Q S and Chai X Y 2013 *Journal of Neuroengineering and Rehabilitation* **10** 1-12
- [12] Ballini M, Muller J, Livi P, Chen Y H, Frey U, Stettler A, Shadmani A, Viswam V, Jones I L, Jackel D, Radivojevic M, Lewandowska M K, Gong W, Fiscella M, Bakkum D J, Heer F and Hierlemann A 2014 *IEEE Journal of Solid-State Circuits* **49**, 2705-2719
- [13] Delivopoulos E, Chew D J, Minev I R, Fawcett J W and Lacour S P 2012 *Lab on a Chip* **12** 2540-2551
- [14] Tolstosheeva E, Gonzalez V G, Biefeld V, Kempen L, Mandon S, Kreiter A K and Lang W 2015 *Sensors* **15** 832-854
- [15] Dragas J, Viswam V, Shadmani A, Chen Y H, Bounik R, Stettler A, Radivojevic M, Geissler S, Obien M, Muller J and Hierlemann A 2017 *IEEE Journal of Solid-State Circuits* **52** 1576-1590
- [16] Qiang T, Wang C and Kim N Y 2016 *IEEE Microwave and Wireless Components Letters* **26** 498-500
- [17] Orazem M E and Tribollet B 2008 *Electrochemical Impedance Spectroscopy* (New York: Wiley)
- [18] Jorcin J B, Orazem M E, Pebere N and Tribollet B 2006 *Electrochimica Acta* **51** 1473-1479
- [19] Nick C, Yadav S, Joshi R, Schneider J J and Thielemann C 2015 *Applied Physics Letters* **107** 013101
- [20] Minev I R and Lacour S P 2010 *Applied Physics Letters* **97** 043707
- [21] Harris A R, Morgan S J, Chen J, Kapsa R M I, Wallace G G and Paolini A G 2013 *Journal of Neural Engineering* **10** 016004
- [22] Ledochowitsch P, Yazdan-Shahmorad A, Bouchard K E, Diaz-Botia C, Hanson T L, He J W, Seybold B W, Olivero E, Phillips E A K, Blanche T J, Schreiner C E, Hasenstaub A, Chang E F, Sabes P N and Maharbiz M M 2015 *Journal of Neuroscience Methods* **256** 220-231
- [23] Jorcin J B, Orazem M E, Pebere N and Tribollet B 2006 *Electrochimica Acta* **51** 1473-1479